# Infrared-to-visible upconversion in $Nd^{3+}$-doped chalcohalide glasses

R. Balda,[1,2] M. Sanz,[1] A. Mendioroz,[1] J. Fernández,[1,2] L. S. Griscom,[3] and J.-L. Adam[3]
[1]*Departamento de Fisica Aplicada I, Universidad del País Vasco, Alameda Urquijo s/n, 48013 Bilbao, Spain*
[2]*Centro Mixto CSIC-UPV/EHU, Universidad del País Vasco, Alameda Urquijo s/n, 48013 Bilbao, Spain*
[3]*Laboratoire des Verres & Céramiques, Université de Rennes 1, UMR-CNRS 6512, Campus de Beaulieu, 35042 Rennes Cedex, France*
(Received 21 March 2001; revised manuscript received 25 May 2001; published 17 September 2001)

The infrared to visible upconversion processes have been investigated for $Nd^{3+}$-doped chalcohalide glasses with different halide modifiers by using steady-state and time-resolved laser spectroscopy. Two different upconversion mechanisms have been identified depending on the infrared excitation wavelength. When the excitation wavelength is resonant with the $^4F_{3/2}$ state, three main bands at 538, 600, and 675 nm are observed and attributed to emissions from the $^4G_{7/2}$ level. These upconverted emissions occur via energy-transfer upconversion involving two neodymium ions in the $^4F_{3/2}$ state. However, nonresonant excitation at higher energies than that of $^4F_{3/2}$ state (between states $^4F_{3/2}$ and $^4F_{5/2}$) or in resonance with the $^4F_{5/2}$ state, causes an additional blue emission to originate from the $^2P_{1/2}$ state. This latter upconverted emission can be attributed to excited-state absorption of the pump radiation. The proposed upconversion mechanisms responsible for the different emissions from levels $^2P_{1/2}$ and $^4G_{7/2}$ are supported by both the time evolution of the upconversion luminescence after infrared pulsed excitation and the upconversion luminescence excitation spectra.

DOI: 10.1103/PhysRevB.64.144101 PACS number(s): 78.20.−e, 78.55.Hx, 78.47.+p

## I. INTRODUCTION

Neodymium has been recognized as one of the most efficient rare-earth (RE) ions for solid-state lasers in different hosts[1,2] due to its intense emission at 1.06 $\mu$m. Recent spectroscopic results have shown that the $Nd^{3+}$ ion could be also considered as a good candidate for upconversion fluorescence and lasers.[3–6] Upconversion fluorescence from $Nd^{3+}$ in glasses has been reported in different hosts.[7–11] Room temperature ultraviolet upconversion with 866-nm pumping for $Nd^{3+}$-activated fluoroindate glass has been reported by Menezes *et al.*[9] Ultraviolet (381-nm) laser action has been demonstrated in Nd-doped ZBLAN glass fiber after excitation at 590 nm at room temperature.[12] In order to investigate new upconversion materials with high luminescence efficiency, hosts with low phonon energies are required. Currently RE-doped fluoride and chalcogenide glasses are the best candidates. The advantage of chalcogenide glasses (sulfide, selenide, and telluride glasses) over the more extensively studied fluoride compounds is the lower phonon energy[13] (less than 400 $cm^{-1}$), which leads to a significant reduction of the multiphonon relaxation rates. This allows an increased lifetime of some excited levels that can relax radiatively or can store energy for further upconversion, cross-relaxation, or energy-transfer processes. For example, the lifetime of the $^4G_{7/2}$ state of $Nd^{3+}$ ions was found to range from 70 ps in oxides to 41 ns in fluoride matrices,[14] whereas in chalcogenide glasses[15] it is around 6 $\mu$s. The chalcogenide glasses present a high refractive index ($>2$), a high spontaneous emission probability and, consequently, large emission cross sections of radiative transitions between energy levels of rare-earth ions. These properties lead to high radiative emission rates of rare-earth energy levels, so that efficient upconversion luminescence intensities can be obtained. Chalcogenide glasses based on sulfides have attracted considerable attention as new optical-fiber materials.[16] Their suitability to be obtained in fiber form has been demonstrated,[17,18] and laser action in neodymium-doped sulfide glass in bulk[19] and fiber[18] has been recently reported in gallium-lanthanum-sulfide glass. $Ga_2S_3$-$Na_2S_3$-based glasses are thermally stable and can also be drawn into fibers. GNS:$Pr^{3+}$ is the first sulfide-glass-fiber amplifier showing gain at 1.3 $\mu$m.[20] Among many sulfide glasses, the germanium-gallium-sulfide (GGS) glass system has been studied for its potential as a low phonon energy glass for lasers and fiber-optic amplifier applications.[21–24] Sulfide glasses, however, usually show a low-energy band gap that causes strong absorption of visible light, as in Ga-and Ge-based glasses,[25,26] which can limit applications such as upconversion. This drawback is partly circumvented in Ge-Ga-S ternary glasses by incorporating a cesium halide. Thus, addition of chlorine, bromine, or iodine ions results in a decrease of sulfur concentration within the glass and a consequent shift of the visible transparency towards shorter wavelengths. This extended transmission in the UV/visible region is advantageous for effective pumping of active ions in the visible and may also allow efficient upconversion processes. In addition, large cations such as cesium, act as network modifiers and open the tetrahedral structure of GGS glass. Therefore, the degree of disorder is higher in the GGS-Cs$X$ ($X$=Cl, Br, I) system and more stable glasses are formed if compared to GGS.[27] It has been also found that Cs$X$ can be introduced with no significant reduction of the infrared transparency and rare-earth solubility in these chalcohalide glasses.

In this work we report the spectroscopic properties and infrared (IR) to visible frequency upconversion mechanisms in $Nd^{3+}$-doped chalcohalide glasses of composition $50GeS_2$-$25Ga_2S_3$-25Cs$X$ ($X$=Cl, Br, I) by using steady-state and time-resolved laser spectroscopy. The study includes one-photon (*OP*) absorption and emission spectroscopy and lifetime measurements for the visible and infrared fluorescence, and IR to blue, green, orange, and red upconversion processes. Two different upconversion mechanisms, depend-

 

ing on the infrared excitation wavelength, have been identified in the two-photon processes involved in the visible luminescence. The presence of blue emission is associated with an excited-state absorption of pump radiation, whereas green, orange, and red emissions are attributed to an energy-transfer upconversion process.

## II. EXPERIMENTAL TECHNIQUES

Chalcohalide glasses were prepared from high-purity ($5N$) germanium and gallium ingots and sulfur chips, along with cesium halides ($3N$), which were weighed in a low-humidity argon-atmosphere glove box. The elements were batched into a silica ampoule, which was then pumped under vacuum to $10^{-4}$ Torr. Finally, the ampoule was sealed using an oxyacetylene torch.

Once sealed, the ampoule was protected with a grille and placed in a tubular oven equipped with a rocking apparatus to better mix the constituents at the reaction temperature. Pure-sulfide samples are usually heated to the reaction temperature at a very slow rate, typically 0.5 to 1.0 °C $\mathrm{min}^{-1}$ to avoid explosion due to unreacted-sulfur-gas phases. Halide-modified glass compositions were found to react more quickly than pure sulfide compounds allowing heating rates of 3 °C $\mathrm{min}^{-1}$.

Once the reaction temperature was reached, rocking for at least 6 h mixed the constituents. The reaction temperature was 925 °C for all glasses. The temperature of the synthesis oven was then reduced (typically 700 °C) and the oven was held in a vertical position with the rocking stopped before quenching. This allowed the glass to settle, minimizing bubbles and composition microinhomogeneities. Finally, the samples were quenched in air for about 30 s and annealed at the glass-transition temperature for several hours.

The composition $50GeS_2$-$25Ga_2S_3$-$25CsX$ ($X=\mathrm{Cl, Br, I}$) was found to give the most thermally stable glasses. For simplicity, the glasses will be coded GGSC, GGSB, and GGSI in the text. $Nd^{3+}$ ions doping is achieved by substituting $\frac{1}{2}Nd_2S_3$ for the whole glass composition to 0.5% of $Nd^{3+}$ in the three glasses.

The samples temperature was varied between 4.2 and 300 K with a continuous-flow cryostat. Conventional absorption spectra were performed with a Cary 5 spectrophotometer. Emission measurements were made using an Argon laser and a Ti: sapphire ring laser (0.4 $\mathrm{cm}^{-1}$ linewidth) in the 780–920 nm spectral range. The fluorescence was analyzed with a 0.25-m monochromator, and the signal was detected by a Hamamatsu R928 photomultiplier and finally amplified by a standard lock-in technique.

Lifetime measurements were obtained by exciting the samples with a dye laser pumped by a pulsed nitrogen laser and a Ti:sapphire laser pumped by a pulsed frequency doubled Nd:YAG laser (9 ns pulse width), and detecting the emission with a Hamamatsu R928 photomultiplier. Data were processed by a Tektronix oscilloscope.

## III. EXPERIMENTAL RESULTS

### A. Continuous-wave excitation

Conventional absorption spectra were performed for the three glasses in the 400–2600 nm spectra range using a Cary 5 spectrophotometer. As an example Fig. 1 shows the absorption spectrum for GGSB glass in the 400–950 nm range at 10.8 K. As can be observed, even at low temperature, levels with higher energies than $^2P_{1/2}$ lie in the absorption edge of the glass. If we compare the room-temperature absorption spectra for the different halide modifiers (Fig. 2), the absorption band gap for GGSB and GGSC glass is similar and is blueshifted with respect to GGSI glass. It is also noticeable that the $Nd^{3+}$ absorption bands for the CsCl-modified glass are blueshifted and their oscillator strengths reduced if compared with the other glasses. This behavior is due to the smaller polarizability of the chloride ligands around the $Nd^{3+}$ ions[28] (a higher ionicity of the glass matrix).

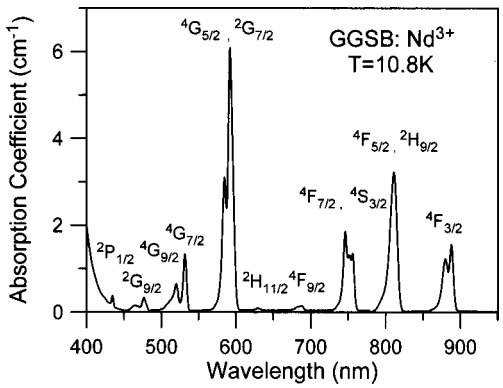


FIG. 1. Absorption spectrum for GGSB glass doped with 0.5% of $Nd^{3+}$ obtained at 10.8 K.

Visible upconversion has been observed in the three glasses under continuous-wave (cw) and pulsed-laser excitation. The upconverted emission spectra obtained under cw IR excitation were measured by using a Ti:sapphire ring laser (0.4 $\mathrm{cm}^{-1}$ linewidth) in the 780–920 nm spectral range. Cut-off filters were used to remove both the pumping radiation and the infrared luminescence from the samples. As an example Fig. 3 shows the upconversion fluorescence spectra for GGSB glass doped with 0.5% of Nd ions in the 400–700 nm region at 77 K obtained by exciting the $^4F_{3/2}$ and $^4F_{5/2}$ multiplets. Figure 3(a) shows the spectrum obtained by exciting at 888 nm in resonance with the $^4I_{9/2} \rightarrow {}^4F_{3/2}$ transition, where three bands located at 538, 600, and 675 nm can

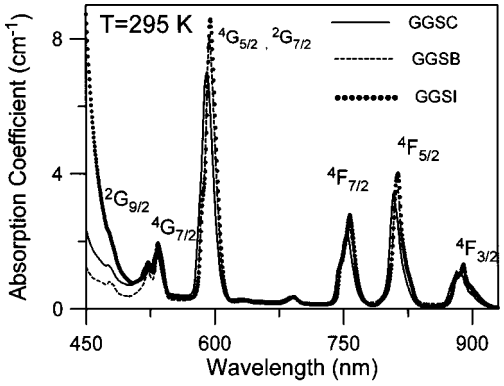


FIG. 2. Room-temperature absorption spectra for GGSC, GGSB, and GGSI glasses doped with 0.5% of $Nd^{3+}$.

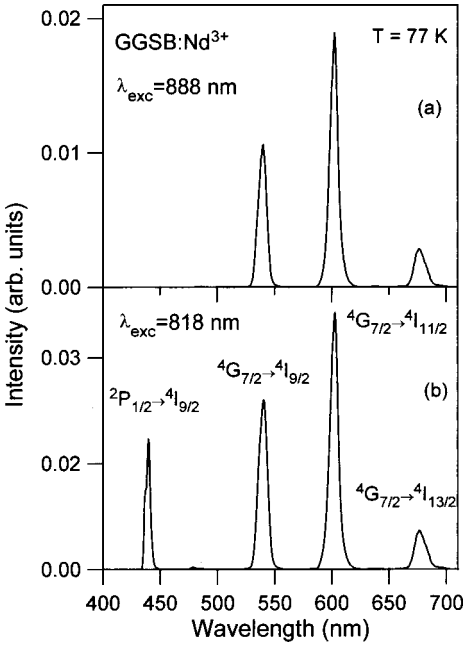


FIG. 3. Emission spectra obtained under excitation (a) at 888 nm in resonance with the $^4F_{3/2}$ level and (b) at 818 nm in resonance with the $^4F_{5/2}$ level for glass GGSB doped with 0.5 mol % of $Nd^{3+}$ ions. Data correspond to 77 K.

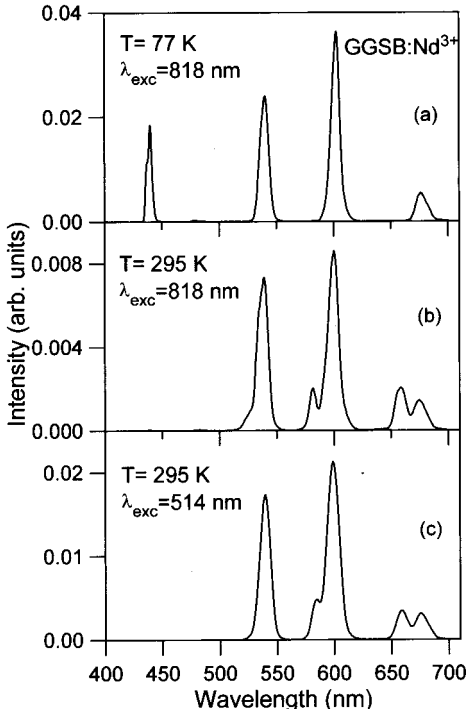


FIG. 4. Emission spectra obtained (a) under excitation at 818 nm in resonance with the $^4F_{5/2}$ level at 77 K, (b) at 818 nm at 295 K, and (c) at 514 nm and 295 K for glass GGSB doped with 0.5 mol % of $Nd^{3+}$ ions.

be observed. As we shall see, these bands correspond to transitions from the $^4G_{7/2}$ level. However, if excitation is performed in resonance with the $^4I_{9/2} \rightarrow {}^4F_{5/2}$ transition, a new band appears around 438 nm, as shown in Fig. 3(b), which is assigned to the $^2P_{1/2} \rightarrow {}^4I_{9/2}(438\,\text{nm})$ transition.

For comparison, Figs. 4(a) and 4(b) show the upconverted emission spectra obtained at 77 and 295 K, respectively, by exciting at 818 nm in resonance with the $^4F_{5/2}$ state. As can be observed at room temperature only the green, orange, and red emissions are observed, and each band contains two components. The extinction of the blue emission at room temperature is probably due to the shift in the absorption edge (450 nm). It is worthy to notice that the high-energy component of the visible bands disappears at 77 K. This demonstrates that the green, orange, and red transitions are originated from two closely spaced levels ($\Delta E \approx 400\,\text{cm}^{-1}$), the higher-energy level being populated through thermalization processes. These closely spaced levels could be ($^4G_{7/2}$-$^4G_{9/2}$) or ($^2G_{9/2}$-$^4G_{11/2}$). The absorption spectroscopy reveals an energy difference of 435 and 635 $\text{cm}^{-1}$ for the ($^4G_{7/2}$-$^4G_{9/2}$) and ($^2G_{9/2}$-$^4G_{11/2}$) levels, respectively. On the other hand, the OP emission spectrum obtained by pumping the $^4G_{9/2}$ level at 514 nm directly [Fig. 4(c)], is found to be similar to that in Fig. 4(b), which suggests that ($^4G_{7/2}$-$^4G_{9/2}$) are the emitting levels for the green, orange, and red transitions. In addition, as we shall see, decay measurements yield similar lifetimes for these emissions, indicating that they originate from the same level or group of levels. In conclusion, green, orange, and red emissions occur from ($^4G_{7/2}$-$^4G_{9/2}$) only, and emission bands correspond to the radiative transitions $^4G_{7/2} \rightarrow {}^4I_{9/2}(538\,\text{nm})$, $^4G_{7/2} \rightarrow {}^4I_{11/2}(600\,\text{nm})$, and $^4G_{7/2} \rightarrow {}^4I_{13/2}(675\,\text{nm})$. Similar upconverted emission spectra are found for different halide (Cl, Br, I) modifiers; however the highest intensity for the blue emission corresponds to GGSC glass and decreases in the Cl-Br-I series, probably due to the shift in the absorption band gap to longer wavelengths, specially in the sample modified with CsI. The extended transmission in the visible region for GGSC and GGSB if compared with the sample modified with CsI may increase the efficiency of the upconversion process involving the $^2P_{1/2}$ level.

To investigate the excitation mechanisms for populating the $^2P_{1/2}$ and $^4G_{7/2}$ levels after IR excitation, we have obtained the evolution of the upconverted emission intensities for different pumping powers. Upconversion intensities were recorded at 438, 538, 600, and 675 nm for different pump powers. Figure 5 shows, as an example, a logarithmic plot of the integrated emission intensity of the upconverted fluorescence at 438 and 538 nm as a function of the pump-laser intensity for GGSB glass. The dependence of the intensity of the three lines (green, orange, and red) on the pump power is nearly quadratic (slope 1.7) for all samples, which indicates a two-photon upconversion process. The same behavior is observed for the blue emission from level $^2P_{1/2}$, which confirms that a two-photon upconversion process is also responsible for the blue emission.

To further investigate the nature of the upconversion processes in these glasses, excitation spectra of the upconverted emissions at 438, 538, 600, and 675 nm were performed at 77 and 295 K in the spectral ranges corresponding to the $^4I_{9/2} \rightarrow {}^4F_{5/2}$ and $^4I_{9/2} \rightarrow {}^4F_{3/2}$ transitions. Figure 6 shows the excitation spectra for the upconverted emissions by monitor-

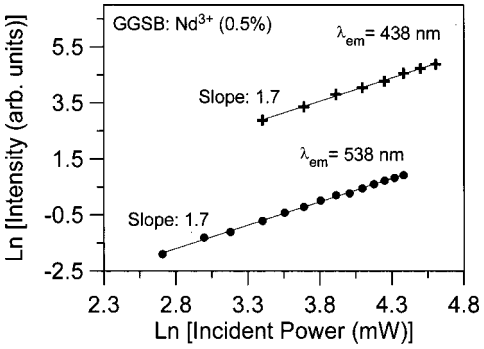


FIG. 5. Logarithmic plot of the integrated intensities of the upconverted emission from $^2P_{1/2}$(438 nm) and $^4G_{7/2}$(538 nm) levels obtained under IR excitation in resonance with $^4F_{5/2}$ level for GGSB glass.

ing the $^2P_{1/2} \rightarrow {}^4I_{9/2}$ transition at 438 nm and the $^4G_{7/2} \rightarrow {}^4I_{9/2}$ transition at 538 nm for GGSB glass doped with 0.5% of $Nd^{3+}$ ions at 77 K, together with the OP absorption spectrum for comparison. Some differences can be observed between the excitation spectrum for blue and green emissions. The spectrum corresponding to the green emission shows two excitation peaks similar to those observed in the absorption spectrum. The first one at 818 nm corresponds to excitation of the ($^4F_{5/2}$, $^2H_{9/2}$) levels, while the second one at 888 nm corresponds to the $^4F_{3/2}$ doublet. Identical excitation spectra were recorded by monitoring either the green, orange, or red emission. However, the excitation spectrum

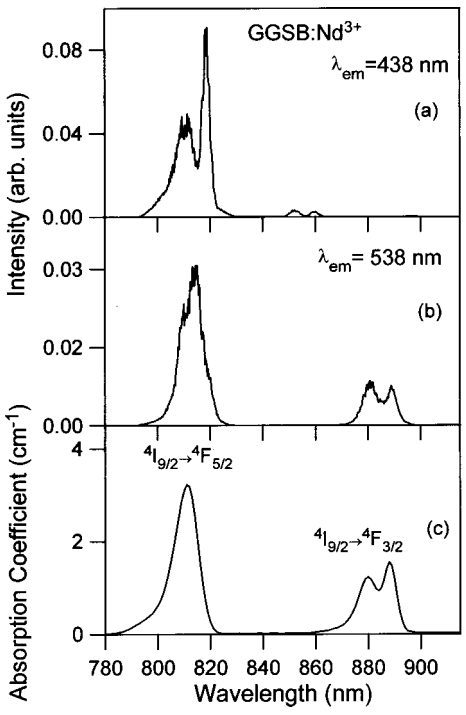


FIG. 6. Excitation spectra of the upconverted emission from (a) $^2P_{1/2}$(438 nm) and (b) $^4G_{7/2}$(538 nm) for GGSB glass doped with 0.5 mol % obtained at 77 K, corrected for the spectral variation of the laser intensity. The one-photon absorption spectrum (c) is also included for comparison.

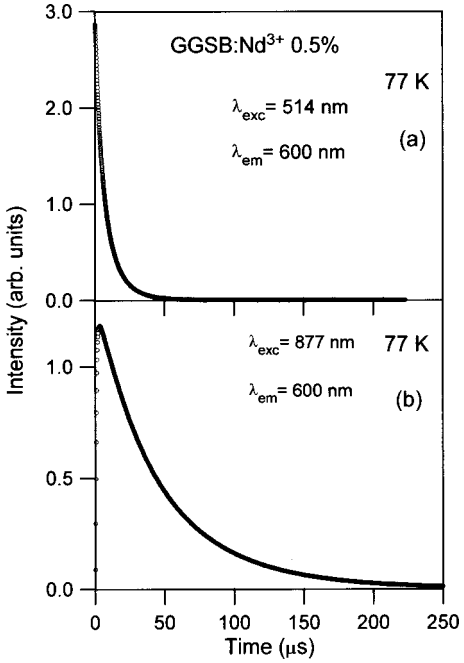


FIG. 7. Experimental emission decay curves of the orange emission (600 nm) from level $^4G_{7/2}$ obtained under excitation (a) at 514 nm and (b) at 877 nm for GGSB glass doped with 0.5 mol % of $Nd^{3+}$. Data correspond to 77 K.

for the intense blue emission at 438 nm exhibits a strong two-component excitation band in the 810–820 nm region, which corresponds to pumping into the ($^4F_{5/2}$, $^2H_{9/2}$) group of levels. It is noteworthy that the blue emission at 438 nm cannot be observed with excitation into $^4F_{3/2}$ that is at ≈888 nm. However, a weak excitation process is observed at around 850 and 860 nm that is in-between the $^4F_{3/2}$ and $^4F_{5/2}$ levels. The upconverted emission spectra obtained by exciting at 850 or 860 nm show an intense blue emission corresponding to the $^2P_{1/2}$ level and the three bands corresponding to the $^4G_{7/2}$ level populated nonradiatively from the $^2P_{1/2}$ level. The reason for this assignment can be found in the lifetime measurements of the involved levels and will be discussed in Sec. IV.

### B. Lifetime measurements

The temporal evolution of the upconverted emissions and the infrared emission of the $^4F_{3/2} \rightarrow {}^4I_{11/2}$ transition were obtained by exciting the samples in resonance with the $^4F_{3/2}$ level at 877 nm and nonresonantly at 860 nm, with a Ti:sapphire laser pumped by a frequency-doubled pulsed Nd:YAG laser. The decays and lifetimes of the $^2P_{1/2}$ and $^4G_{7/2}$ levels were also obtained for all samples under direct excitation with a dye laser. Similar temporal evolutions are observed for the green, orange, and red emissions. As an example Fig. 7 shows the experimental decays of the orange emission obtained at 77 K by exciting at 514 and 877 nm for GGSB glass doped with 0.5 mol % of $Nd^{3+}$ ions. As can be observed, the decay curve of the upconverted emission shows a lifetime longer than that of level $^4G_{7/2}$ under direct excitation. Table I presents the lifetime values of this level for the

TABLE I. Lifetimes ($\mu$s) of the $^4G_{7/2}$ level obtained under direct excitation (514 nm) and infrared excitation (877 nm) for the three glasses doped with 0.5 mol % of $Nd^{3+}$ at 77 K. Lifetimes of the $^4F_{3/2}$ level are also included.

| | $\tau$ ($\mu$s) $^4G_{7/2}$ | | $\tau$ ($\mu$s) $^4F_{3/2}$ |
|---|---|---|---|
| | $\lambda_{exc}=514$ nm | $\lambda_{exc}=877$ nm | $\lambda_{exc}=877$ nm |
| GGSC | 14.4 | 54.5 | 108 |
| GGSB | 13 | 52 | 103 |
| GGSI | 8.4 | 48 | 96 |

three glasses doped with 0.5% of $Nd^{3+}$ obtained under direct and infrared excitations, as well as the lifetime values of the $^4F_{3/2}$ state. The lifetime values correspond to the average lifetime defined by $\tau_{avg}=\int tI(t)dt/\int I(t)dt$. As can be observed, the lifetimes obtained under infrared excitation are around 50 $\mu$s, which are much longer than those obtained under direct pumping and about half the value of the $^4F_{3/2}$ level lifetime. This behavior is in agreement with the predictions of a simple rate-equation model considering a three-level system ($^4I_{9/2}$, $^4F_{3/2}$, and $^4G_{7/2}$) and energy-transfer upconversion (ETU) as the dominant mechanism. This model predicts that the time evolution of the intensity of the upconverted luminescence from the excited $^4G_{7/2}$ level decays with a lifetime, which is half the lifetime value of level $^4F_{3/2}$. Such rate-equation treatment can be found in the literature in reference to different situations.[29,30] The same temporal behavior was observed for the different halide modifiers (Cl, Br, I), but the longer lifetimes correspond to GGSC glass. The trend in the lifetimes for the different halide modifiers is as expected. In general they become longer for glasses with a higher ionicity and a lower index of refraction.[28] In the samples studied the refractive index decreases from 2.0559 for GGSI glass to 2.016 in the case of GGSC glass.

The temporal evolution of the blue emission shows a different behavior. The decay curves obtained under infrared excitation at 860 nm do not show any rise time, and the lifetime is similar to that of level $^2P_{1/2}$ under direct excitation. Figure 8 shows the decays obtained under direct excitation and under IR excitation at 860 nm for GGSB glass. Table II presents the lifetime values of the blue emission after direct excitation and after nonresonant IR excitation at 860 nm for the three glasses.

All the results presented above lead us to point out to the existence of two different mechanisms, depending on the excitation energy, to populate both $^2P_{1/2}$ and $^4G_{7/2}$ levels under IR excitation.

## IV. DISCUSSION

As we have seen in the previous section, two excited levels $^2P_{1/2}$ and $^4G_{7/2}$ are responsible for the observed luminescence at low temperature, whereas only level $^4G_{7/2}$ contributes to the visible luminescence at room temperature. The pumping- power dependence of the upconverted emissions from these levels indicates that a two-photon upconversion process is responsible for the blue emission from level $^2P_{1/2}$ and the green, orange, and red emission from $^4G_{7/2}$ level. This process may be associated to excited state absorption (ESA) involving single ions and/or ETU involving two excited ions.[31,32] It is well established that the upconversion luminescence excitation spectra and the temporal evolution of the upconversion luminescence after pulsed excitation allow to distinguish between ESA and ETU processes.[5,33] In the case of ETU, the excitation spectrum is proportional to the square of the OP absorption coefficient as a function of wavelength, as the initial excited population is excited by OP absorption from a monochromatic source and is proportional to the OP absorption coefficient. On the other hand, in the case of excited-state absorption, two transitions, the OP absorption and ESA transition, must occur at the same wavelength for excitation to take place. As a consequence, the upconversion excitation spectrum is the result of OP absorption and excited-state absorption. Therefore, peaks in the OP absorption spectrum may not appear in the excitation spectrum if there is no or little ESA at the same wavelength.[5,33]

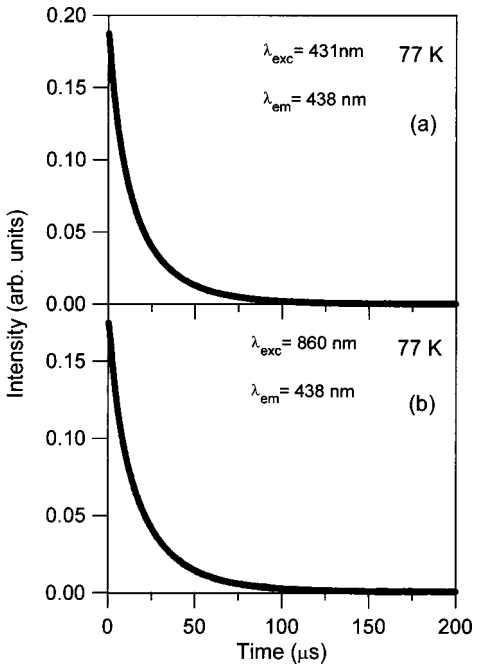


FIG. 8. Experimental emission decay curves of the blue emission from level $^2P_{1/2}$ obtained under excitation (a) at 431 nm and (b) at 860 nm for GGSB glass doped with 0.5 mol % of $Nd^{3+}$. Data correspond to 77 K.

TABLE II. Lifetimes ($\mu$s) of the $^2P_{1/2}$ level obtained under OP excitation (431 nm) and under nonresonant infrared excitation (860 nm) for the three glasses doped with 0.5 mol % of $Nd^{3+}$ at 77 K.

| | Lifetime ($\mu$s) $^2P_{1/2}$ | |
|---|---|---|
| | $\lambda_{exc}=431$ nm | $\lambda_{exc}=860$ nm |
| GGSC | 18 | 19 |
| GGSB | 16.5 | 17 |
| GGSI | 13 | 13.5 |

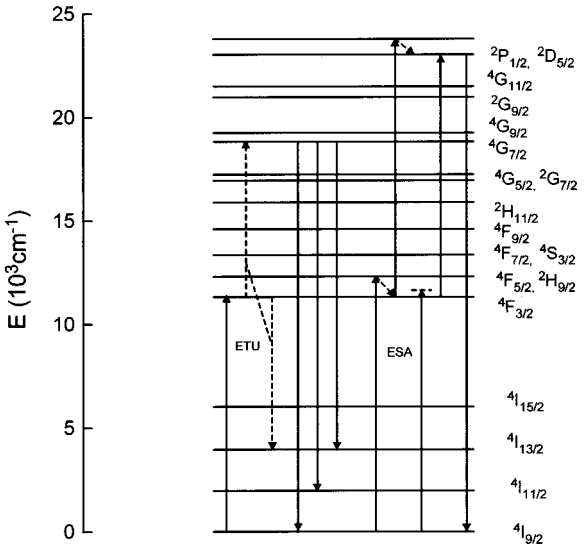


FIG. 9. Energy-level diagram of $Nd^{3+}$ in GGSB glass and the proposed upconversion mechanisms to populate $^2P_{1/2}$ and $^4G_{7/2}$ levels after IR excitation.

Clearly, the excitation spectra for the blue and for the green, orange, and red emissions show a different behavior. In the first case, the excitation spectra do not follow the square of the OP absorption coefficient. Some of the OP absorption peaks do not appear in the upconversion excitation spectra. This indicates that ESA is the dominant mechanism for the 438-nm blue emission obtained under 818-nm excitation and observed at low temperature, which is assigned to the $^2P_{1/2} \rightarrow {}^4I_{9/2}$ transition and can be explained by the pumping mechanisms described in Fig. 9. In a first step the absorption of one IR pump-photon excites the electrons to the $(^4F_{5/2}, {}^2H_{9/2})$ multiplet, then multiphonon relaxation occurs to the $^4F_{3/2}$ doublet, and subsequently ESA of a second 818-nm pump photon promotes the electrons to the $^2D_{5/2}$ level and, finally, by nonradiative relaxation $^2P_{1/2}$ level is reached. This blue emission is also observed under nonresonant excitation at higher energies than that of $^4F_{3/2}$ state. In this process a $Nd^{3+}$ ion in its ground state absorbs an IR photon nonresonantly and ends up in the $^4F_{3/2}$ state assisted by a phonon emission. Then a second IR photon is resonantly absorbed and reaches level $^2P_{1/2}$ directly (Fig. 9).

The excitation spectra of the upconverted green, orange, and red emissions, follow the same wavelength dependence as the OP absorption spectra, which indicates that we are dealing with an ETU to populate the $^4G_{7/2}$ state. From the energy levels of $Nd^{3+}$ in these glasses, the most likely resonant-energy-transfer process to populate the $^4G_{7/2}$ level after the absorption of one infrared photon is $(^4F_{3/2}, {}^4F_{3/2}) \rightarrow (^4I_{13/2}, {}^4G_{7/2})$ (Fig. 9). In this process, when two $Nd^{3+}$ ions are excited by an IR photon directly to the $^4F_{3/2}$ state or by fast relaxation from the $^4F_{5/2}$ state depending on the excitation energy, a transfer occurs by which, one ion loses energy and goes to the $^4I_{13/2}$ state while the other one gains energy and goes to the $^4G_{7/2}$ state.

A further support to this hypothesis is given by lifetime measurements. The time evolution of the upconversion luminescence after an excitation pulse provides a useful tool in discerning which is the operative mechanism. The radiative ESA process occurs during the excitation pulse width, and leads to an immediate decay of the upconversion luminescence after excitation. Upconversion by energy transfer leads to a decay curve for the upconversion emission, which shows a rise time after the laser pulse, followed by a decay and lifetime longer than that after direct excitation. The rise and decay times are determined by both the intermediate and the upper excited-state lifetimes. This distinction is possible when the pulse width is much shorter than the time constant of the relevant energy-transfer step.[5] The time evolution of the decays from the $^4G_{7/2}$ level obtained after an infrared excitation pulse of 9 ns clearly follows the latter behavior. As shown in Fig. 7, after IR excitation in the $^4F_{3/2}$ state the decay curve of the upconverted fluorescence shows a rise time and a lifetime longer than that of level $^4G_{7/2}$ under OP excitation, which indicates that the energy-transfer process is responsible for the green, orange, and red emission. The lifetime values of the $^4G_{7/2}$ level is about half the lifetimes of the $^4F_{3/2}$ state, which indicates that the upconversion emission from level $^4G_{7/2}$ is caused by interaction between two $Nd^{3+}$ ions in the $^4F_{3/2}$ level (ETU) and not by excited-state absorption.[5,33] In the case of excited-state absorption the lifetime values under OP and TP excitation should be the same.

The temporal evolution of the blue emission follows a different behavior. As shown in Fig. 8, after nonresonant-pulsed infrared excitation between the $^4F_{3/2}$ and $^4F_{5/2}$ states, the resulting $^2P_{1/2} \rightarrow {}^4I_{9/2}$ upconversion luminescence intensity decays instantaneously after the laser pulse and the lifetime is similar to that of the $^2P_{1/2}$ excited level under direct excitation. The same result is obtained by resonant excitation in the $^4F_{5/2}$ band. Therefore, we conclude that the infrared-to-blue upconversion mechanism is the ESA process displayed in Fig. 9. Moreover, the lifetime values of the $^4G_{7/2}$ level obtained under excitation at 850 or 860 nm are the same as those obtained under OP direct excitation of level $^2P_{1/2}$; therefore, the presence of an ETU mechanism, involving the $^4F_{3/2}$ level, to populate the $^4G_{7/2}$ level can be disregarded. On the other hand, taking into account the energy difference between the peak positions of the two small excitation peaks [850 and 860 nm, respectively in Fig. 6(a)], which is similar to the splitting of the $^4F_{3/2}$ doublet ($\approx$110 $cm^{-1}$), and considering the energy-level diagram shown in Fig. 9, the possible ESA transition giving rise to the blue emission should be $^4F_{3/2} \rightarrow {}^2P_{1/2}$. As $^2P_{1/2}$ is a singlet level, the energy matching for the ESA process can be obtained from the low-energy component of the $^4F_{3/2}$ doublet for the 850-nm excitation peak, whereas the 860-nm peak could be associated with ESA involving the high-energy component of level $^4F_{3/2}$. The weak intensity of these two bands is due to the low probability of reaching the high $^4F_{3/2}$ energy side bands from the ground state.

It is worthy to mention that the proposed upconversion mechanisms for the population of the $^2P_{1/2}$ and the $^4G_{7/2}$ states are in agreement with both the upconversion-luminescence excitation spectra and the time-dependent results. The same behavior is observed for the different halide modifiers.

Finally, if we compare the upconversion mechanisms observed in these chalcohalide glasses with those observed in other $Nd^{3+}$-doped materials, in particular, with fluoride and chloride hosts, one of the differences is the absence of blue and ultraviolet emissions originated from the $^4D_{3/2}$, $^4D_{5/2}$, $^4D_{1/2}$ levels populated by a three-photon process[9,10,30] after infrared excitation. As we mentioned before, in these chalcohalide glasses the observed strong blue emission is only due to the $^2P_{1/2}$ level populated by a two-photon process because $Nd^{3+}$ energy levels above the $^2P_{1/2}$ singlet lie in the absorption edge of the glass host. Referring to the green, orange, and red emissions obtained after infrared excitation, all of them have been observed in other materials and attributed to an energy-transfer process involving two $Nd^{3+}$ ions excited in the $^4F_{3/2}$ state.[5,11,30] However, the room-temperature upconversion efficiency of these visible emissions from $^4G_{7/2}$ level is higher by a factor of 40 in chalcohalide glasses if compared with that in fluoride-based glasses. This comparison has been performed with a $Nd^{3+}$-doped ZBLAN glass by exciting both glasses with the same energy in the same region of the $^4F_{3/2}$ band at wavelengths that gave the same absorption coefficient for both samples and keeping the same experimental conditions. The same result for the upconversion efficiency was obtained by exciting in the $^4F_{5/2}$ band. The higher efficiency of chalcohalide glasses is due to their lower phonon energies, which reduce the nonradiative rates from the emitting levels.

## V. CONCLUSIONS

Infrared-to-visible upconversion in $Nd^{3+}$-doped chalcohalide glasses has been investigated under continuous-wave and pulsed-laser excitation for different halide modifiers. Similar upconverted emission spectra are found with different halide (Cl, Br, I) modifiers; however glass modified with CsCl shows the highest intensity for the blue emission. This emission decreases in the Cl-Br-I series probably due to a shift in the absorption bandgap to longer wavelengths, specially in the sample modified with CsI.

The analysis of the experimental results as a function of excitation wavelength, pumping power, and time shows the existence of two different upconversion mechanisms (ESA and ETU) to populate both $^2P_{1/2}$ and $^4G_{7/2}$ states. The study of upconversion processes has shown that infrared excitation at 888 nm in the $^4F_{3/2}$ level leads to green, orange, and red emissions from the ($^4G_{7/2}$-$^4G_{9/2}$) levels. The excitation-wavelength dependence of the green, orange, and red emissions together with the time evolution of the decays suggest that an ETU process involving two $Nd^{3+}$ ions in the $^4F_{3/2}$ state is responsible for these emissions from level $^4G_{7/2}$. For blue upconversion from level $^2P_{1/2}$ an ESA is suggested as the main mechanism to populate $^2P_{1/2}$ after IR excitation in resonance with the $^4F_{5/2}$ or after nonresonant excitation between the $^4F_{3/2}$ and $^4F_{5/2}$ states.

The comparison of the upconversion efficiency between $Nd^{3+}$-doped chalcohalide and fluoride (ZBLAN) glasses, shows that visible emission intensities are about 40 times higher for the chalcohalide materials.

## ACKNOWLEDGMENTS

This work has been supported by the Ministerio de Ciencia y Tecnología (Ref. BFM2000-0352 and French-Spanish PICASSO Program No. HF 99/43) and Basque Country University (Ref. G21/98).

[1] A. A. Kaminskii, in *Laser Crystals*, 2nd ed., edited by D. L. MacAdam, Springer Series in Optical Sciences Vol. 14 (Springer-Verlag, Berlín, 1990).
[2] M. J. Weber, J. Non-Cryst. Solids **123**, 208 (1990).
[3] S. Guy, M. F. Joubert, B. Jacquier, and M. Bouazaoui, Phys. Rev. B **47**, 11 001 (1993).
[4] Y. Guyot, H. Manna, J. Y. Rivoire, R. Moncorgé, N. Garnier, E. Descroix, M. Bon, and P. Laporte, Phys. Rev. B **51**, 784 (1995).
[5] D. S. Wenger, D. R. Gamelin, H. U. Güdel, A. V. Butashin, and A. A. Kaminskii, Phys. Rev. B **61**, 16 530 (2000).
[6] R. M. McFarlane, F. Fong, A. J. Silversmith, and W. Lenth, Appl. Phys. Lett. **52**, 1300 (1988).
[7] T. Stanley, E. A. Harris, T. M. Searle, and J. M. Parker, J. Non-Cryst. Solids **161**, 235 (1993).
[8] T. Tsuenoka, K. Kojima, and S. Bojja, J. Non-Cryst. Solids **202**, 297 (1996).
[9] L. de S. Menezes, Cid B. de Araujo, G. S. Maciel, Y. Messaddeq, and M. A. Aegerter, Appl. Phys. Lett. **70**, 683 (1997).
[10] G. S. Maciel, L. de S. Menezes, C. B. de Araujo, and Y. Messadeq, J. Appl. Phys. **85**, 6782 (1999).
[11] R. Balda, J. Fernández, M. Sanz, A. de Pablos, J. M. Fdez-Navarro, and J. Mugnier, Phys. Rev. B **61**, 3384 (2000).
[12] D. S. Funk, J. M. Carlson, and J. G. Eden, Electron. Lett. **30**, 1859 (1994).
[13] P. N. Kumta and S. H. Risbud, J. Mater. Sci. **29**, 1135 (1994).
[14] S. A. Payne and C. Bibeau, J. Lumin. **79**, 143 (1998).
[15] T. Schweizer, in *Properties, Processing and Applications of Glass and Rare-earth Doped Glasses for Optical Fibers*, edited by D. Hewak (INSPEC, London, 1998), Vol. 22, p. 320.
[16] J. S. Sanghera and I. D. Aggarwal, J. Non-Cryst. Solids **256&257**, 6 (1999).
[17] D. W. Hewak, R. C. Moore, T. Schweizer, J. Wang, B. Samson, W. S. Brocklesby, D. N. Payne, and E. J. Tarbox, Electron. Lett. **32**, 384 (1996).
[18] T. Schweizer, B. N. Samson, R. C. Moore, D. W. Hewak, and D. N. Payne, Electron. Lett. **33**, 414 (1997).
[19] T. Schweizer, D. W. Hewak, D. N. Payne, T. Jensen, and G. Huber, Electron. Lett. **32**, 666 (1996).
[20] H. Tawarayama, in *Properties, Processing and Applications of Glass and Rare-earth Doped Glasses for Optical Fibres* (Ref. 15), p. 355.
[21] Y. Ohishi, A. Mori, T. Kanamori, K. Fujiura, and S. Sudo, Appl. Phys. Lett. **65**, 13 (1994).
[22] D. R. Simons, A. J. Faber, and H. de Waal, J. Non-Cryst. Solids **185**, 283 (1995).

[23] K. Wei, D. P. Machewirth, J. Wenzel, E. Snitzer, and G. H. Sigel, Jr., J. Non-Cryst. Solids **182**, 257 (1995).
[24] K. Abe, H. Takebe, and K. Morinaga, J. Non-Cryst. Solids **212**, 143 (1997).
[25] D. J. Brady, *Properties, Processing and Applications of Glass and Rare-earth Doped Glasses for Optical Fibres* (Ref. 15), p. 293.
[26] Y. Guimond, J. L. Adam, A. M. Jurdyc, J. Mugnier, B. Jacquier, and X. H. Zhang, Opt. Mater. **12**, 467 (1999).
[27] L. S. Griscom, J. L. Adam, and K. Binnemans, J. Non-Cryst. Solids **256&257**, 383 (1998).
[28] M. J. Weber, D. C. Ziegler, and C. A. Angell, J. Appl. Phys. **53**, 4344 (1982).
[29] B. R. Reddy and P. Venkateswarlu, J. Chem. Phys. **79**, 5845 (1983).
[30] T. Chuang and H. R. Verdún, IEEE J. Quantum Electron. **32**, 79 (1996).
[31] F. Auzel, Proc. IEEE **61**, 758 (1973).
[32] J. C. Wright, Top. Appl. Phys. **15**, 239 (1976).
[33] T. Y. Fan and R. L. Byer, J. Opt. Soc. Am. B **3**, 1519 (1986).